JASA ARTICLE

Laryngeal strategies to minimize vocal fold contact pressure and their effect on voice production

Zhaoyan Zhang[a)]
Department of Head and Neck surgery, University of California, Los Angeles, 31-24 Rehabilitation Center, 1000 Veteran Avenue, Los Angeles, California 90095-1794, USA

ABSTRACT:
The goal of this study is to identify laryngeal strategies that minimize vocal fold contact pressure while producing a target sound pressure level (SPL) using a three-dimensional voice production model. The results show that while the subglottal pressure and transverse stiffness can be manipulated to reduce the peak contact pressure, such manipulations also reduce the SPL, and are thus less effective in reducing contact pressure in voice tasks targeting a specific SPL level. In contrast, changes in the initial glottal angle and vocal fold vertical thickness that reduce the contact pressure also increase the SPL. Thus, in voice tasks targeting a specific SPL, such changes in the initial glottal angle and vertical thickness also lower the subglottal pressure, which further reduces the peak contact pressure. Overall the results show that for voice tasks with a target SPL level, vocal fold contact pressure can be significantly reduced by adopting a barely abducted glottal configuration or reducing the vocal fold vertical thickness. Aerodynamic measures are effective in identifying voice production with large initial glottal angles, but by themselves alone are not useful in differentiating hyperadducted vocal folds from barely abducted vocal folds, which may be better differentiated by closed quotient and voice type measures. © *2020 Acoustical Society of America*. https://doi.org/10.1121/10.0001796

(Received 7 June 2020; revised 3 August 2020; accepted 6 August 2020; published online 26 August 2020)
[Editor: James F. Lynch] Pages: 1039–1050

I. INTRODUCTION

During human phonation the vocal folds almost always experience repeated collision as the glottis periodically opens and closes. For very loud or prolonged voice production, the resulting contact pressure between the vocal folds may lead to vocal fold tissue injury, which, if not mitigated, may further develop into vocal fold lesions such as vocal fold nodules, polyps, or contact ulcers (Hillman *et al.*, 1989). Understanding how the contact pressure varies with the geometric and mechanical properties of the vocal system would allow us to avoid vocal behaviors that likely result in high vocal fold contact pressure and thus high risk of vocal fold injury, and adopt vocal behaviors that minimize contact pressure when meeting a target vocal demand, which has important applications in voice therapy and voice training (Peterson *et al.*, 1994; Titze, 2006).

The goal of this study is to identify laryngeal strategies that minimize vocal fold contact pressure when producing a target sound pressure level (SPL), and their acoustic, aerodynamic, and vibratory impact. This study is a follow-up to a previous computational study (Zhang, 2019). Using a three-dimensional computational voice production model, Zhang (2019) conducted a large-scale computational study of voice production with parametric variations in vocal fold approximation, vocal fold medial surface vertical thickness, transverse and longitudinal stiffness in the body and cover layers of the vocal fold, subglottal pressure, and vocal tract configuration. The results showed that the subglottal pressure and transverse stiffness of the vocal fold have the largest and most consistent effect on the peak contact pressure over the range of voice conditions investigated, with the peak contact pressure consistently increasing with increasing subglottal pressure or decreasing transverse stiffness. In contrast, the effect of changes in other vocal fold properties such as vocal fold approximation and medial surface vertical thickness on vocal fold contact pressure is less consistent and varies depending on values of other vocal fold properties and vocal tract configurations.

One deficiency of the Zhang (2019) study is that the effect of changes in vocal fold properties on voice production, particularly the SPL, was not considered. It is possible that changes in certain vocal fold properties reduces vocal fold contact pressure at the cost of reduced SPL, and thus are not very effective in minimizing vocal fold contact pressure in voice tasks demanding a specific SPL. For example, while Zhang (2019) showed that reducing the subglottal pressure significantly decreases the peak contact pressure, such reduction in subglottal pressure also significantly decreases SPL, and thus is not an effective option to reduce contact pressure when a specific SPL is desired. In contrast, vocal fold properties with a less consistent global effect on contact pressure (e.g., vertical thickness) may be more effective in minimizing contact pressure if changes in these parameters reduce the peak contact pressure and increase SPL simultaneously.

Furthermore, by focusing on the global trends across a large number of vocal fold conditions, Zhang (2019) did not investigate potential local minima of the contact pressure at intermediate values of vocal fold properties. It is possible

[a)]Electronic mail: zyzhang@ucla.edu, ORCID: 0000-0002-2379-6086.

that the less consistent effect of medial surface thickness and the initial glottal angle observed in the study by Zhang (2019) was due to a nonlinear relationship between these parameters and vocal fold contact pressure. Indeed, it has been shown that optimal vocal efficiency is obtained at an intermediate degree of vocal fold adduction, also referred to as a flow phonation configuration (Gauffin and Sundberg, 1989). Berry *et al.* (2001) demonstrated in their excised larynx experiment the existence of a minimum of vocal fold contact pressure at conditions with a 0.5 mm distance between the vocal processes. Clinically, voice therapies targeting on vocal fold nodules often aim for a barely abducted or barely adducted laryngeal configuration to minimize vocal fold contact pressure [e.g., Peterson *et al.* (1994), Verdolini-Marston *et al.* (1995), and Verdolini *et al.* (1998)]. Understanding how the peak contact pressure varies with the initial glottal angle and medial surface vertical thickness would also allow us to examine potential compensation strategies in response to vocal fold injury, providing a scientific foundation for current and new voice therapy approaches.

The specific goals of this study are to (1) investigate the general trends of how changes in vocal fold geometric and mechanical properties affect vocal fold contact pressure and vocal intensity and (2) identify laryngeal strategies that would minimize vocal fold contact pressure in voice tasks targeting a specific SPL. Considering the potential nonlinear dependence of the contact pressure on the glottal gap reported in the literature, we expanded the range of initial glottal angles from that in Zhang (2019) to include two extreme conditions representing medial compression of the vocal folds and glottal insufficiency with a large initial glottal angle. Due to the difficulty of directly measuring vocal fold contact pressure in live humans, quantitative voice output measures that differentiate different laryngeal strategies are of particular clinical interest [e.g., Hillman *et al.* (1989), Peterson *et al.* (1994), and Holmberg *et al.* (2003)]. Therefore, a third goal of this study is to identify the acoustic, aerodynamic, and vibratory impact of different laryngeal strategies to minimize vocal fold contact pressure. In the following, the computational model, simulation conditions, and data analysis are first described in Sec. II. The results are presented in Sec. III, followed by discussions in Sec. IV.

II. METHOD

A. Computational model and simulation conditions

The same three-dimensional vocal fold model as in the study by Zhang (2019) was used in this study. The reader is referred to these previous studies for details of the model (Zhang, 2015, 2017, 2019). A sketch of the vocal fold model is shown in Fig. 1. Left-right symmetry in vocal fold properties (geometry, material properties, and position) about the glottal midline is imposed so that only one vocal fold is modeled in this study. The vocal fold cross-section tapers quadratically toward the anterior direction, with the total medial-lateral depth reduced by half from the posterior surface to the anterior surface of the vocal folds. The vocal fold model is fixed at the lateral surface and the two side surfaces at the anterior and posterior ends. Each vocal fold layer is modeled as a transversely isotropic, nearly incompressible, linear material with a plane of isotropy perpendicular to the anterior-posterior (AP) direction. The material control parameters for each vocal fold layer include the transverse Young's modulus E_t, the AP Young's modulus E_{ap}, the AP shear modulus G_{ap}, and density. The glottal flow is modeled as a one-dimensional quasi-steady glottal flow model taking into consideration viscous loss, as described in detail in Zhang (2015, 2017). Vocal fold contact occurs when portions of the vocal fold cross the glottal midline, in which case a penalty pressure along the medial-lateral direction into the vocal fold is applied to the contact surface of the vocal fold (Zhang, 2015, 2019). A large enough penalty pressure will ensure small penetration depth of the vocal folds crossing the glottal midline, and the corresponding penalty pressure will approximate the true contact pressure (Wriggers, 2006; Zhang, 2019). Our previous studies using similar computational models have been able to predict voice production by unsteady glottal flow (Zhang *et al.*, 2002), phonation threshold pressure and frequency in a two-layer silicone vocal fold model (Farahani and Zhang, 2016), and vocal fold vibration patterns in different vibratory regimes and transitions between regimes (Zhang and Luu, 2012).

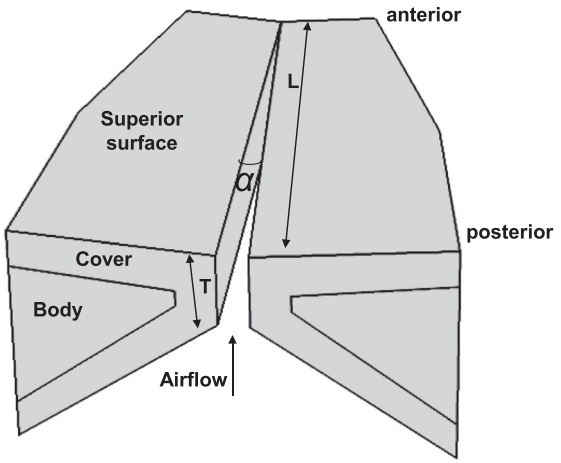

FIG. 1. The three-dimensional vocal fold model and key geometric control parameters, including the vocal fold length L along the anterior-posterior direction, vertical thickness of the medial surface T, and the initial glottal angle α.

The model is parameterized by various geometric and mechanical properties of the vocal folds. In this study, as in the study by Zhang (2019), parametric variations in the following six model control parameters were considered: the vocal fold medial surface vertical thickness T, the initial glottal angle α (for which the vertex is the anterior commissure) controlling the degree of vocal fold approximation, vocal fold transverse Young's modulus E_t, vocal fold longitudinal shear moduli in the body and cover layers G_{apb} and G_{apc}, and subglottal pressure P_s. The parametric values used

https://doi.org/10.1121/10.0001796

for these model parameters in this study are listed in Table I, based on previous experimental and computational studies (Hollien and Curtis, 1960; Titze and Talkin, 1979; Hirano and Kakita, 1985; Isshiki, 1989; Alipour-Haghighi and Titze, 1991; Alipour *et al.*, 2000; Zhang *et al.*, 2017). Geometrically, the vertical thickness of the medial surface in the superior-inferior direction T was varied between 1 and 4.5 mm. Our previous studies have shown that this range of vertical thickness can produce voice qualities varying from breathy, modal, pressed, to irregular voice as the vertical thickness is increased (Zhang, 2016, 2018). Previously in the study by Zhang (2019), only positive values of the initial glottal angle α, which controls the degree of vocal fold approximation, were considered. In the present study, we expanded the range of the initial glottal angle α to −1.6°, 0°, 1.6°, 4°, 8°, with the negative value simulating conditions of medial compression of the vocal folds. This range corresponds to an inter-vocal process distance between −0.5 and 2.4 mm, which is similar to that investigated in previous excised larynx experiments (Jiang and Titze, 1994; Berry *et al.*, 2001). Mechanically, the transverse stiffness of both layers E_t was varied from 1 to 2 and 4 kPa. The AP shear moduli in the cover and body layers, G_{apc} and G_{apb}, were each varied from 1, 10, 20, 30, to 40 kPa, thus generating a total of 25 unique (G_{apc}, G_{apb}) conditions. The subglottal pressure was varied between 0 and 2.4 kPa, a total of 18 conditions that covers the range from soft voice to very loud voice. The simulation was performed for two vocal tract conditions, corresponding to the /ɑ/ or /i/ sounds, which have a high and low first formant, respectively. The vocal tract is modeled as a one-dimensional waveguide (Story, 1995), and the cross-sectional area functions reported in Story *et al.* (1996) were used.

The other model control parameters were kept constant in this study, including the vocal fold length along the AP direction of 17 mm, a medial-lateral depth of 6 and 1.5 mm in the body and cover portions, respectively, of the posterior cross-section of the vocal folds. The depth of the cover layer was gradually reduced superiorly and inferiorly and was set to be constant at 0.5 mm at the superior and inferior ends of the cover layer, based on measurements in Wu and Zhang (2016). The medial surface forms an initial uniform vertical glottal angle of zero degrees with the vertical axis. More details of the geometric control of the model can be found in Zhang (2017; Fig. 1). The density of the vocal fold was assumed to be 1030 kg/m^3. The AP Poisson's ratio was assumed to be 0.495. As in previous studies (Zhang, 2017, 2018), to reduce the number of conditions to be investigated, the AP Young's modulus E_{ap} was assumed to be four times the AP shear modulus G_{ap}, and the transverse Young's moduli of the two layers were assumed to be identical in the present study. For both layers, a constant loss factor of 0.4 was used, similar to Zhang (2016).

TABLE I. Ranges of model control parameters. For all conditions, the vocal fold density is 1030 kg/m^3, the AP Poisson's ratio is 0.495, and $E_{ap} = 4\,G_{ap}$ is assumed.

Transverse Young's modulus	$E_t = [1, 2, 4]$ kPa
Cover AP shear modulus	$G_{apc} = [1, 10, 20, 30, 40]$ kPa
Body AP shear modulus	$G_{apb} = [1, 10, 20, 30, 40]$ kPa
Vertical thickness	$T = [1, 2, 3, 4.5]$ mm
Initial glottal angle	$\alpha = [-1.6°, 0°, 1.6°, 4°, 8°]$
Subglottal pressure	$P_s = 50$–2400 Pa (18 conditions)
Vocal tract	/ɑ/, /i/

In total, 27 000 conditions were investigated for each vocal tract condition, with a total of 54 000 conditions. For each condition, a half-second of voice production was simulated at a sampling rate of 44 100 Hz, with the subglottal pressure linearly increased from zero to a target value in 30 time steps (about 0.68 ms) and then kept constant.

B. Data processing

For each phonating condition, the peak contact pressure over the medial surface was calculated using the last 0.25 s of each simulation, by which time vocal fold vibration had either reached steady state or nearly steady state. For each condition, the fundamental frequency F0 and A-weighted SPL were extracted as described in Zhang (2016). Cepstral peak prominence (CPP) (Hillenbrand *et al.*, 1994) and harmonic-to-noise ratio (HNR) were also extracted from the voice acoustics. The closed quotient (CQ) of vocal fold vibration was calculated as the fraction of the cycle in which the glottal area function falls within the lower 10% between the minimum and maximum glottal area. The peak-to-peak amplitude of the glottal area waveform (Agamp) was also extracted. From the glottal flow waveform, the mean glottal flow rate (Qmean), the peak-to-peak amplitude (Qamp), and the maximum flow declination rate (MFDR) (the most negative peak of the glottal flow derivative) were extracted. For MFDR calculation, the glottal flow waveform was first moving averaged with a window size of four data points (about 0.09 ms) to reduce the noise component present in the flow waveform, which otherwise at conditions of very high flow rate would lead to MFDR occurring at instants of maximum glottal opening rather than at the glottal closing phase. These measures can be obtained relatively easily and were often investigated in previous research toward potentially distinguishing vocal hyperfunction and different phonation modes in voice therapy (Hillman *et al.*, 1989; Peterson *et al.*, 1994; Holmberg *et al.*, 2003). Additionally, from the glottal area waveform, each voice was categorized into three voice types (Titze, 1995): type 1 for regular vocal fold vibration, type 2 for subharmonic vibration, and type 3 for irregular vocal fold vibration, as described in Zhang (2018). Although the thus-obtained voice type is a categorical variable, for convenience it was treated as a numerical variable in the analysis below, with the three voice types 1, 2, and 3 assigned a value of 1, 2, and 3, respectively.

C. Statistical analysis

In our previous study (Zhang, 2019), a histogram analysis was performed to investigate how consistently an increase in a specific control parameter increases or

decreases the peak contact pressure over the entire range of voice conditions investigated. In this study, we performed multi-factorial analysis of variance (ANOVA) to uncover the general trend of variation of the peak contact pressure over the ranges of vocal fold properties and subglottal pressure. Multiple comparisons with Bonferroni correction were made to further evaluate the general trends of variation of the peak contact pressure at different steps of individual control parameters and identify the optimal laryngeal conditions that minimize the peak contact pressure.

Two analyses were performed in this study. First, a multi-factorial ANOVA analysis was performed to the entire dataset to investigate how peak contact pressure and selected output measures vary with different values of the six control parameters. Then, the same analysis was repeated to a subset of conditions that produced a SPL within ±1 dB of a target value to investigate how such constraint of a target SPL affects the effectiveness of different laryngeal strategies in reducing the peak contact pressure. We considered a target SPL of 60, 70, and 80 dB for conditions with the /i/ vocal tract, and a target SPL of 70, 80, and 90 dB for condition with the /ɑ/ vocal tract. These values were determined from the SPL range in our data and reflected the differences in the radiation efficiency between the two vocal tract configurations. Under the constraint of producing a target SPL level, the six control parameters were no longer independent. As this study focused on laryngeal strategies and considering the large effect of the subglottal pressure on the peak contact pressure, we considered the subglottal pressure as a dependent variable that needs to be adjusted according to settings of the other five control parameters in order to produce a target SPL level. Therefore, a multi-factorial ANOVA analysis was then performed with the five control parameters (the original six controls excluding the subglottal pressure) as independent factors.

Initially the ANOVA analysis was performed including both the main effect and two-way interactions. Including higher-order interactions was not possible due to the fact that we had only one sample for each combination of control parameters and some combinations did not produce sustained phonation and thus had no data. One typical result is shown in Table II, with the peak contact pressure as the dependent variable and the six control parameters as independent factors and using the entire dataset. All main effects and interactions were significant with $p < 0.005$. We notice that the interaction terms generally had smaller F values than the main effects, with a few exceptions. Unfortunately, the subsets of conditions that produced a given target SPL level often included only a few hundred conditions, which are too few to estimate even two-way interactions. For a fair comparison of results between the entire dataset and the subsets producing a specific SPL, we decided to use the same statistical model including only main effects for both analyses. Considering the lack of systematic understanding of how contact pressure and other output measures vary with the control parameters, it seems logical to focus in this study on the overall trends of each individual control parameter before taking on their complex interactions. Thus, for clarity of presentation, in the following only results from statistical models with main effects only are presented, with the understanding that the F values and effect sizes may be slightly under- or over-estimated.

TABLE II. F values and effect sizes η^2 of the six control parameters and two-way interactions in ANOVA analysis of the peak contact pressure over all conditions with the /ɑ/ vocal tract.

	F	η^2		F	η^2
P_s	1835	0.295	T*α	28	0.003
T	67	0.002	T*E_t	73	0.004
α	1820	0.069	T*G_{apc}	130	0.015
E_t	412	0.008	T*G_{apb}	100	0.011
G_{apc}	504	0.019	α*E_t	452	0.034
G_{apb}	668	0.025	α*G_{apc}	249	0.038
P_s*T	15	0.007	α*G_{apb}	75	0.011
P_s*α	32	0.020	E_t*G_{apc}	36	0.003
P_s*E_t	159	0.051	E_t*G_{apb}	151	0.011
P_s*G_{apc}	8	0.005	G_{apc}*G_{apb}	79	0.012
P_s*G_{apb}	36	0.023			

III. RESULTS

A. Overall trends of the peak contact pressure

Table III shows the results from the ANOVA analysis of the peak contact pressure P_c and SPL over all phonating conditions, for both vocal tract configurations. All main effects were significant with $p < 0.005$. Figures 2 and 3 (upper left panel) further show the average values of the peak contact pressure as a function of the initial glottal angle for different values of the vertical thickness and transverse stiffness, respectively. Note that the mean peak contact pressures in Figs. 2 and 3 are larger than those reported in previous experiments [e.g., Jiang and Titze (1994) and Verdolini *et al.* (1999)]. This is because our simulations included conditions of very large subglottal pressure and low transverse stiffness, which significantly increased the overall average of the peak contact pressure across all conditions.

For both vocal tract configurations, the subglottal pressure, initial glottal angle, and transverse stiffness had the largest effect size on the peak contact pressure. Specifically, the peak contact pressure increased with increasing subglottal pressure or decreasing transverse stiffness, which is consistent with the findings in the study by Zhang (2019). The large effect size of the initial glottal angle and the relatively small effects size of the transverse stiffness [compared to that in Zhang (2019)] were largely due to the newly added condition of $\alpha = -1.6°$, which simulates medial compression of the vocal folds and was not included in the Zhang (2019) study. Excluding conditions with the negative initial glottal angle significantly reduced the effect size of the initial glottal angle to below about 0.02 and increased the effect size of the transverse stiffness to above 0.1 (also see

https://doi.org/10.1121/10.0001796

TABLE III. F values, effect size η^2, and multiple comparison (MC) results from ANOVA analysis of the peak contact pressure P_c and SPL over the entire dataset. All effects were significant for $p < 0.005$. Control parameters with opposite effects on the contact pressure and SPL are highlighted in bold. The inequality symbols (<, >) indicate significant multiple comparison results with $p < 0.005$.

			P_s	T (mm)	α (deg.)	E_t (kPa)	G_{apc} (kPa)	G_{apb} (kPa)
/ɑ/	P_c	F/η^2	1048/0.394	**125/0.008**	**1404/0.124**	1611/0.071	210/0.019	581/0.051
		MC	increase w/ P_s	**1 < 2 < 3 < 4.5**	**0 < 1.6 < 4 < 8 < −1.6**	1 > 2 > 4	20 > (10,30) > 40 > 1	1 < 10 < (20,30,40)
	SPL	F/η^2	2733/0.651	**272/0.011**	**595/0.033**	1346/0.038	250/0.014	391/0.022
		MC	increase w/ P_s	**1 > (2, 3) > 4.5**	**1.6 > 0 > 4 > −1.6 > 8**	1 > 2 > 4	(10,20) > 30 > 40 > 1	1 < 10 < (20,30,40)
/i/	P_c	F/η^2	1002/0.347	**30/0.002**	**2366/0.193**	1334/0.054	87/0.007	634/0.052
		MC	increase w/ P_s	**1 < (2, 3, 4.5)**	**0 < 1.6 < (4, 8) < −1.6**	1 > 2 > 4	20 > (10,30) > 40 > 1	1 < 10 < (20,30,40)
	SPL	F/η^2	2846/0.671	**744/0.031**	**352/0.020**	1010/0.028	206/0.011	239/0.013
		MC	increase w/ P_s	**1 > 2 > 3 > 4.5**	**1.6 > 0 > 4 > (8, −1.6)**	1 > 2 > 4	(10,20) > 30 > 40 > 1	1 < 10 < (20,30,40)

Fig. 3), which is consistent with the observation in Zhang (2019). Multiple comparison showed that the contact pressure reached the minimum at the initial glottal angle of 0° and increased as the initial glottal angle deviated from this optimal value, which is shown more clearly in Fig. 2 (first panel). Note that interaction between the initial glottal angle and vertical thickness can be observed in Fig. 2, in which the optimal glottal angle becomes 1.6° for conditions with a 4.5 mm thickness.

Changes in the body-layer AP stiffness G_{apb} also had notable effects on the peak contact pressure, with an effect size around 0.05 for both vocal tract configurations (Table III). However, the effect was statistically significant only between the smaller stiffness values (1 and 10 kPa) and larger values but not between any of the large stiffness conditions (20, 30, 40 kPa). This is consistent with the generally small effect of AP stiffness observed in our previous studies [e.g., Zhang (2017)]. The effect sizes of the vertical thickness and cover-layer AP stiffness were even smaller. Multiple comparisons showed that the peak contact pressure increased with either increasing vertical thickness or increasing body-layer AP stiffness. The peak contact pressure reached maximum at intermediate values of the cover-layer AP stiffness, although the effect size was small.

Table III also shows how the SPL varied with the six control parameters. As expected, the subglottal pressure had

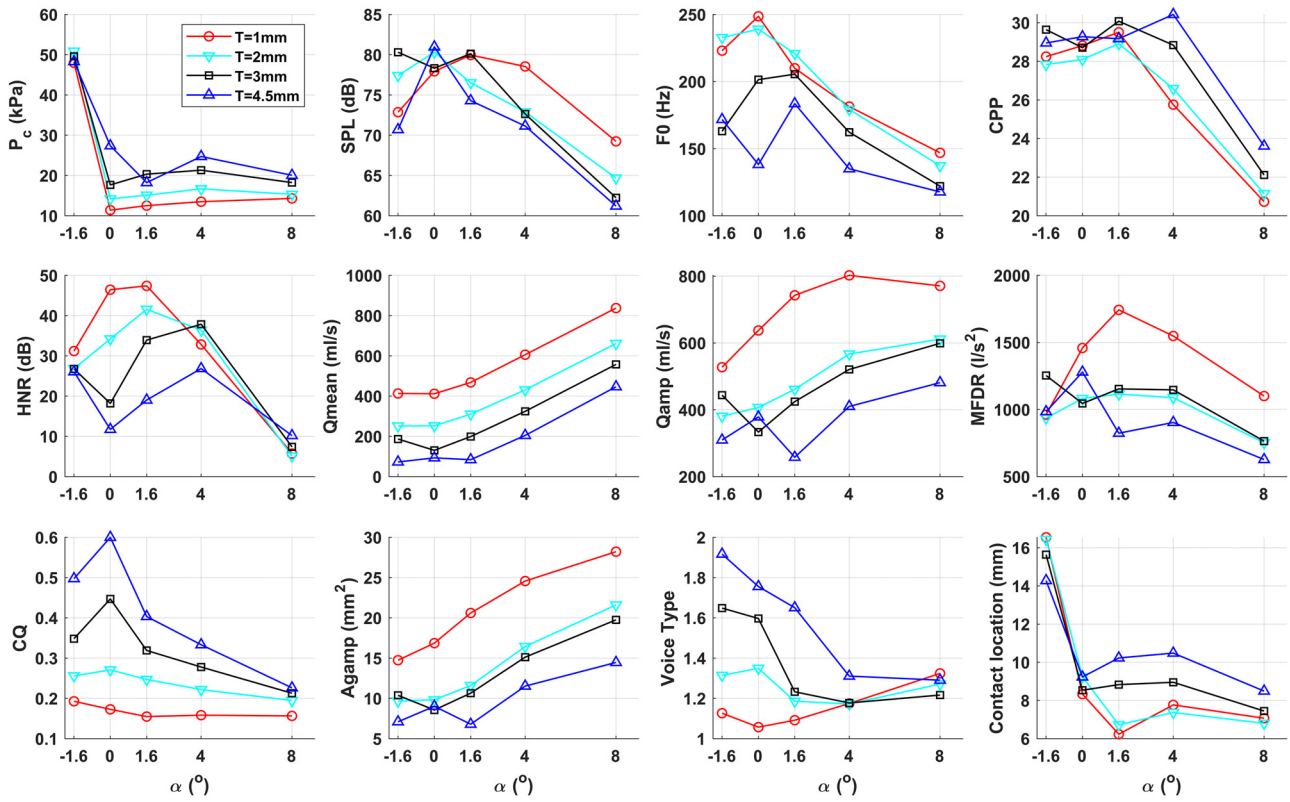

FIG. 2. (Color online) For all vocal fold conditions with the /ɑ/ vocal tract. Average values of the contact pressure, selected voice output measures, and AP location of peak contact pressure as a function of the initial glottal angle α for difference values of the medial surface vertical thickness T. High values of the voice type indicate high likelihood for irregular (subharmonic or chaotic) vocal fold vibration. For peak contact location, 0 and 17 mm correspond to the anterior and posterior ends of the vocal fold, respectively.

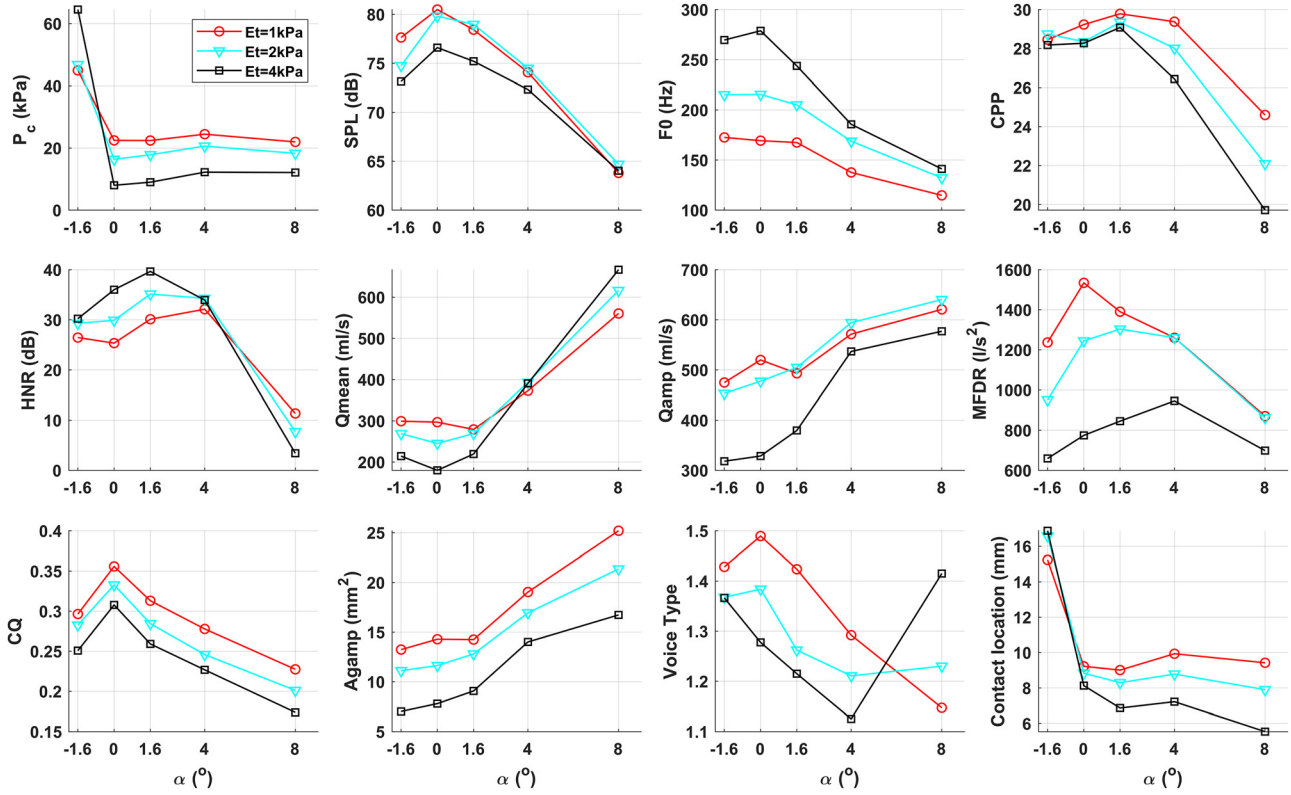

FIG. 3. (Color online) For all vocal fold conditions with the /ɑ/ vocal tract. Average values of the contact pressure, selected voice output measures, and peak contact location as a function of the initial glottal angle α for difference values of the transverse stiffness E_t. High values of the voice type indicate high likelihood for irregular (subharmonic or chaotic) vocal fold vibration.

the largest effect size on the SPL, similar to its dominant effect on the peak contact pressure. A notable observation is that except for the vertical thickness and initial glottal angle, variations in the other control parameters that decreased the peak contact pressure also decreased the SPL, thus making them ineffective in reducing the peak contact pressure while producing a target SPL. For example, although the subglottal pressure had the largest effect size on both the peak contact pressure and SPL, changes in the subglottal pressure required to reduce the peak contact pressure (i.e., a reduction in subglottal pressure) also significantly reduced the SPL, which is undesirable in voice tasks demanding a target SPL level. In contrast, manipulations of the vertical thickness or initial glottal angle led to trends of changes in the peak contact pressure and SPL that were opposite to each other. For example, a decrease in the vertical thickness decreased the peak contact pressure but increased SPL. Thus, for smaller vertical thicknesses, the same SPL can be achieved with less subglottal pressure, which would further reduce the peak contact pressure. This implies that these two parameters may have an increased role in regulating contact pressure in voice tasks demanding a target SPL level such as singing or public speaking, which is discussed below in Sec. III B.

Table IV shows the F values and effect sizes of the six control parameters on other selected output measures and the AP location of the peak contact pressure. All main effects were significant. Figures 2 and 3 also show the average values of these output measures as a function of the initial glottal angle for different values of the vertical thickness and transverse stiffness, respectively. The main effect of increasing subglottal pressure was to increase Qmean, Qamp, Agamp, and MFDR, although it also had moderate effects on F0, CPP, and HNR. In general, increasing the initial glottal angle decreased F0 and voice type (thus less likely of irregular vibration), but increased Qmean, Qamp, and Agamp. For HNR, CPP, MFDR, and CQ, they first increased with increasing initial glottal angle, reached the maximum at an intermediate value before they decreased with further increase in the initial glottal angle. Note that the large effect sizes of the initial glottal angle on CPP and HNR were largely due to significant changes in these output measures at conditions of $\alpha = 8°$, which probably are outside typical ranges of normal phonation [e.g., Isshiki (1989)]. Increasing vertical thickness generally decreased SPL, F0, HNR, Qmean, Qamp, Agamp, MFDR, but increased CPP, CQ, and occurrence of irregular vocal fold vibration (as indicated by increased voice type values). Increasing transverse stiffness increased F0 and HNR, but decreased SPL, CPP, Qmean, Qamp, MFDR, Agamp, CQ, and occurrence of irregular vocal fold vibration (Fig. 3), although some interactions can be observed. These trends are consistent with the results in our previous findings (Zhang, 2016, 2017, 2018) and other studies in the literature [e.g., Herbst *et al.* (2015)].

The peak contact pressure generally occurred at the mid-membranous region (around AP location of 8.5 mm) of

https://doi.org/10.1121/10.0001796

TABLE IV. F values and effect size η^2 of the six control parameters on selected voice output measures and peak contact location, for data in the entire dataset. All effects were significant for $p < 0.005$. Control parameters with an effect size larger than 0.1 are highlighted in bold.

F/η^2		P_s	T	α	E_t	G_{apc}	G_{apb}
/ɑ/	F0	87/0.048	513/0.050	**1281/0.166**	1159/0.075	316/0.041	136/0.018
	CPP	50/0.034	176/0.021	**1234/0.197**	181/0.014	28/0.004	258/0.041
	HNR	25/0.015	458/0.050	**1749/0.255**	57/0.004	36/0.005	253/0.037
	Qmean	**1318/0.300**	**5308/0.213**	**5807/0.311**	482/0.013	96/0.005	925/0.050
	Qamp	**1551/0.530**	1628/0.098	1034/0.083	1144/0.046	392/0.032	60/0.005
	MFDR	**1728/0.579**	700/0.041	176/0.014	1969/0.078	192/0.015	258/0.020
	CQ	23/0.012	**2960/0.283**	**916/0.117**	342/0.022	85/0.011	305/0.039
	Agamp	**767/0.304**	**2169/0.152**	**2013/0.188**	2042/0.095	493/0.046	46/0.004
	VoiceType	14/0.013	210/0.034	62/0.013	29/0.003	11/0.002	56/0.012
	Location	**233/0.130**	272/0.027	**1449/0.190**	906/0.059	58/0.008	225/0.030
/i/	F0	49/0.031	314/0.035	**1029/0.151**	833/0.061	375/0.055	78/0.012
	CPP	102/0.070	294/0.036	**992/0.160**	36/0.003	93/0.015	133/0.021
	HNR	110/0.065	64/0.007	**1927/0.268**	152/0.011	72/0.010	149/0.021
	Qmean	**1568/0.334**	**6894/0.259**	**4839/0.242**	290/0.007	97/0.005	931/0.047
	Qamp	**1949/0.584**	**2100/0.111**	543/0.038	941/0.033	504/0.036	100/0.007
	MFDR	**1537/0.541**	824/0.051	125/0.010	1521/0.063	224/0.019	216/0.018
	CQ	94/0.043	**4336/0.351**	298/0.032	706/0.038	92/0.010	721/0.078
	Agamp	**865/0.334**	**1845/0.126**	**1498/0.136**	**2308/0.105**	892/0.081	123/0.011
	VoiceType	38/0.033	90/0.014	135/0.028	104/0.011	75/0.015	18/0.004
	Location	150/0.078	90/0.008	**2401/0.291**	685/0.042	62/0.007	86/0.010

the vocal folds (Figs. 2 and 3), except for conditions with the negative initial glottal angle for which the peak contact pressure occurred close to the posterior end (17 mm in the last panel of Figs. 2 and 3). The very posterior peak contact location likely resulted from the way medial compression was implemented in this study. Due to the medial rigid-body rotation of the vocal fold, a large penetration depth (about 0.5 mm) was imposed at the posterior end of the vocal fold. Because of the fixed boundary condition at the posterior end, this large penetration cannot be pushed back by the large contact pressure it produced. As a result, a large contact pressure always existed at the posterior end of the vocal folds for $\alpha = -1.6°$. For initial glottal angles large than 0°, the peak contact location moved posteriorly with increasing subglottal pressure. There was also a tendency for the peak contact location to move posteriorly with increasing vertical thickness or decreasing transverse stiffness.

Taken together, Tables III and IV show that very high peak contact pressure can occur at laryngeal conditions of either negative initial glottal angles, small transverse stiffness, or large vertical thickness. For negative initial glottal angles, corresponding to vocal fold medial compression due to for example hyperadduction, the voice is featured with a reduced SPL, reduced mean and peak-to-peak airflow, increased CQ, slightly reduced HNR, and increased occurrence of irregular vocal fold vibration. In contrast, very large initiate glottal angle leads to noticeably reduced F0, SPL, CPP, and HNR, and significantly increased mean and peak-to-peak amplitude of the glottal airflow and area waveforms. The results also showed that extreme thickening of the vocal fold leads to reduced SPL, F0, HNR, Qmean, Qamp, Agamp, MFDR, but increased CQ and occurrence of irregular vocal fold vibration.

B. Voice production with a target SPL level

Considering that manipulations of the vertical thickness T and initial glottal angle α led to changes in the peak contact pressure and SPL of opposite directions, we expect them to be more effective in regulating contact pressure in voice tasks with a target SPL level. Table V shows the F values and effect sizes from the ANOVA analysis applied to vocal fold conditions that produced a target SPL value. As expected, the effect sizes of the initial glottal angle and vertical thickness were much larger than those in Table III without the constraint of a target SPL production. The effect size increased with increasing target SPL level for the vertical thickness, but decreased with the target SPL level for the initial glottal angle. This suggests that manipulation of the vertical thickness is the most effective in reducing the peak contact pressure at high SPL levels, whereas manipulation of the initial glottal angle is the most effective at moderate SPL levels.

The effect size of the transverse stiffness on the other hand was notably reduced compared to that in Table III, except for the highest SPL target levels. In general, the effects of the three stiffness control parameters (E_t, G_{apc}, G_{apb}) on the peak contact pressure were small, except for a moderate effect of the cover-layer AP stiffness for the highest SPL target in /ɑ/.

Multiple comparisons showed that the peak contact pressure decreased with decreasing vertical thickness and reached a minimum at intermediate initial glottal angles of 0° and 1.6°, which is also shown in Fig. 4. Interaction between the initial glottal angle and vertical thickness can be also observed. For example, for conditions with $\alpha = -1.6°$ the average peak contact pressure varied with the vertical thickness in an almost opposite trend from that for

TABLE V. F values, effect size η^2, and multiple comparison (MC) results of the five laryngeal control parameters from ANOVA analysis of the peak contact pressure for conditions producing a target SPL. All effects were significant for $p < 0.005$ unless noted. The inequality symbols (<, >) indicate significant multiple comparison results with $p < 0.005$.

			T (mm)	α (deg.)	E_t (kPa)	G_{apc} (kPa)	G_{apb} (kPa)
/ɑ/	90 dB	F/η^2	233/0.259	234/0.348	88/0.066	31/0.046	11/0.017
		MC	1 < 2 < 3 < 4.5	(0,1.6) < 4 < (−1.6, 8)	1 > 2 > 4	1 < 10 < 30, 1 < (20,40)	1 < (20,30,40), 10 < 40
	80 dB	F/η^2	56/0.082	266/0.524	5/0.005	12/0.024	13/0.026
		MC	1 < (2,3) < 4.5	(0,1.6) < 4 < 8 < −1.6	1 > 4	1 < (20,30,40), 10 < (30,40)	1 < (10,20,30,40)
	70 dB	F/η^2	8/0.018	194/0.589	1[a]/0.002	3[a]/0.010	7/0.022
		MC	(1,2,3) < 4.5	(0,1.6,4) < 8 < −1.6	none	none	1 < (10,20,30,40)
/i/	80 dB	F/η^2	25/0.121	44/0.287	21/0.067	4[a]/0.028	4[a]/0.024
		MC	1 < (2,3) < 4.5	(0,1.6) < 4 < 8, (0,1.6) < −1.6	1 > 2 > 4	none	none
	70 dB	F/η^2	110/0.173	173/0.362	34/0.036	3[a]/0.007	25/0.052
		MC	1 < (2,3) < 4.5	(0,1.6) < 4 < 8 < −1.6	1 > 2 > 4	none	1 < (10,20,30,40)
	60 dB	F/η^2	56/0.066	326/0.513	10/0.008	6/0.010	27/0.042
		MC	1 < (2,3) < 4.5	(0,1.6) < (4,8) < −1.6	1 > 4	1 < 20	1 < (10,20,30,40)

[a]Not significant for $p < 0.005$.

other values of the initial glottal angles. Similar interaction can be also observed between the initial glottal angle and transverse stiffness in Fig. 5 and for conditions with the /i/ vocal tract.

The increase in the effect size for the initial glottal angle and vertical thickness was largely due to the compensatory change in the subglottal pressure that was required to produce the target SPL, as shown in Fig. 4, which shows the average values of the peak contact pressure (first panel, Fig. 4) and subglottal pressure (second panel, Fig. 4) required to produce a target SPL of 80 dB with the /ɑ/ vocal tract. While a deviation from the optimal initial glottal angles (0° and 1.6°) or an increase in the vertical thickness by itself increased the peak contact pressure (first panel, Fig. 2), it also led to compensatory increase in the subglottal pressure (second panel, Fig. 4), which further increased the

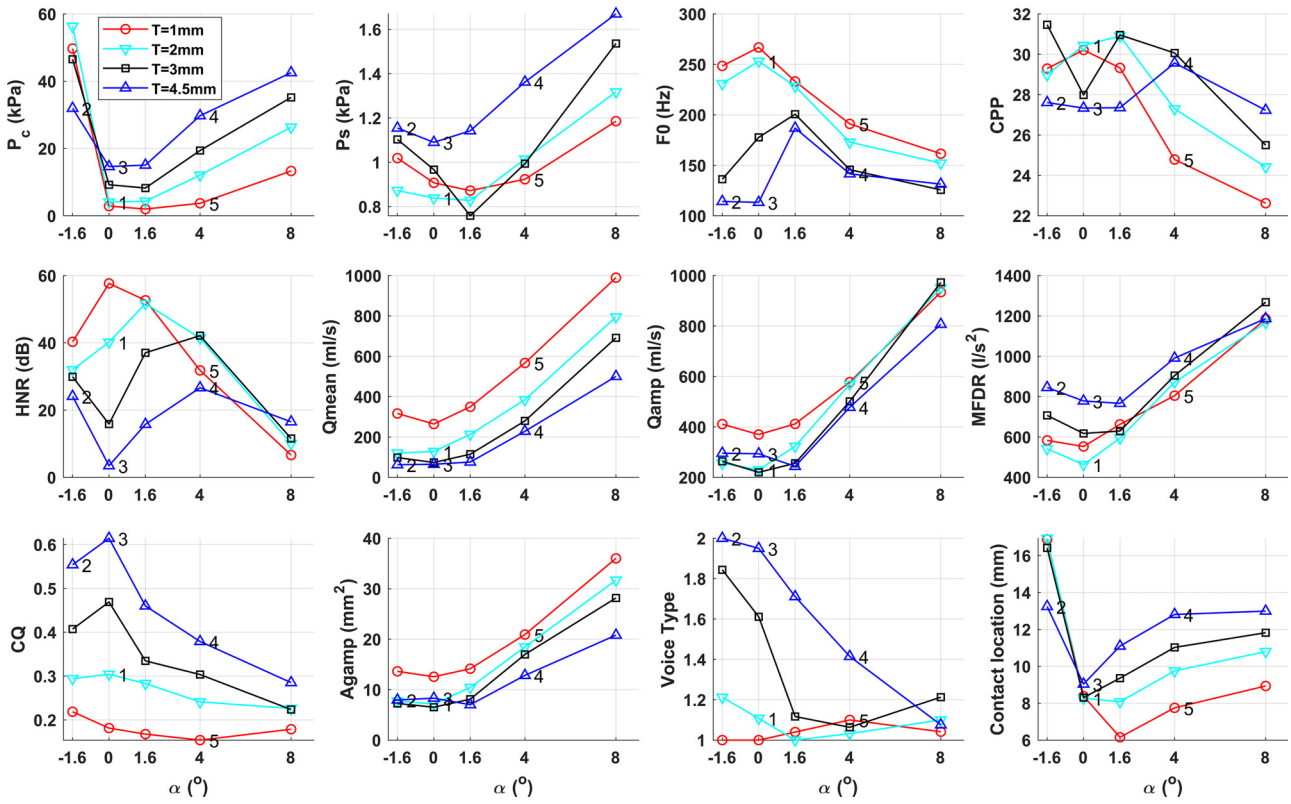

FIG. 4. (Color online) For vocal fold conditions with the /ɑ/ vocal tract and producing an 80 dB SPL. Average values of the contact pressure, subglottal pressure, selected voice output measures, and peak contact location as a function of the initial glottal angle α for difference values of the medial surface vertical thickness T. High values of the voice type indicate high likelihood for irregular (subharmonic or chaotic) vocal fold vibration. The numbers 1–5 indicate the five progressive stages of the development and treatment of vocal fold nodules as discussed in Sec. IV.

https://doi.org/10.1121/10.0001796

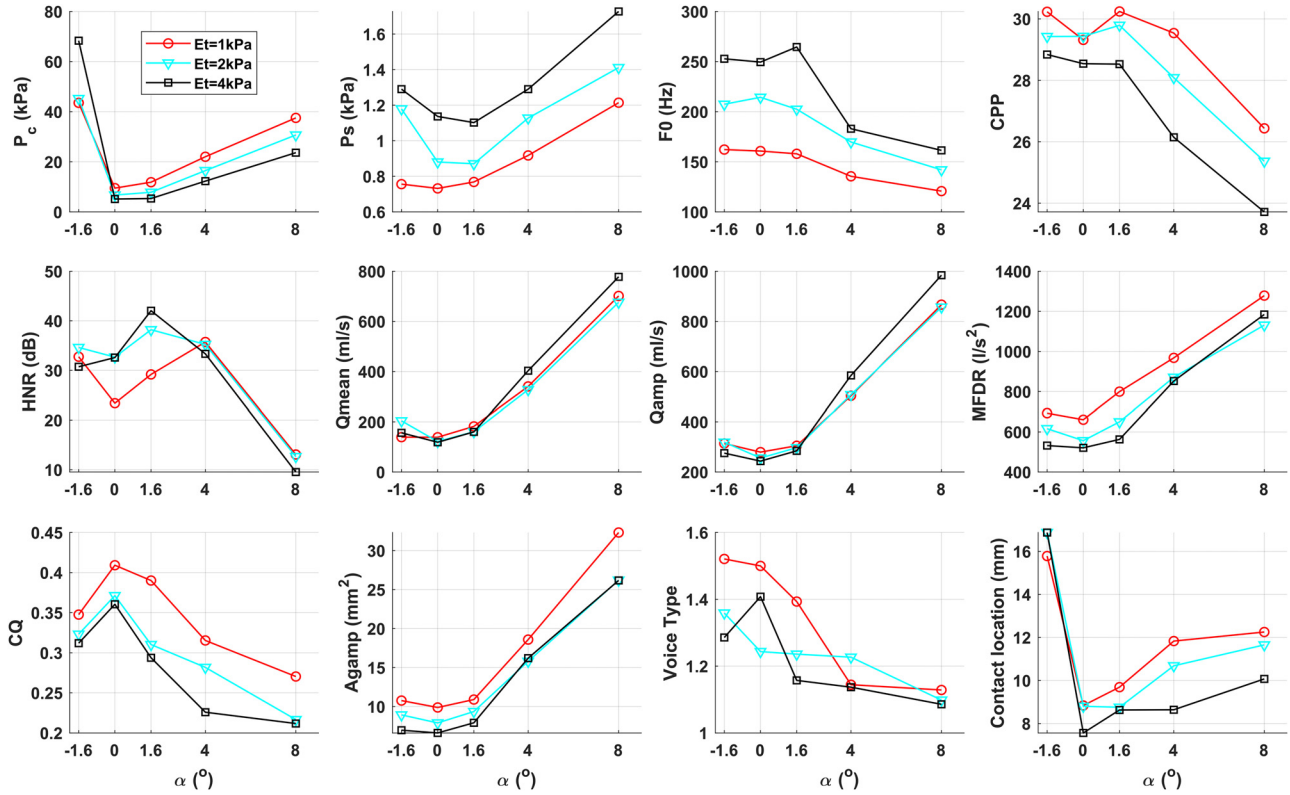

FIG. 5. (Color online) For vocal fold conditions with the /ɑ/ vocal tract and producing an 80 dB SPL. Average values of the contact pressure, subglottal pressure, selected voice output measures, and peak contact location as a function of the initial glottal angle α for difference values of the transverse stiffness E_t. High values of the voice type indicate high likelihood for irregular (subharmonic or chaotic) vocal fold vibration.

peak contact pressure (compare the first panels in Figs. 2 and 4). In contrast, while an increase in the transverse stiffness decreased the peak contact pressure, this effect was partially counteracted by the compensatory increase in the subglottal pressure (second panel, Fig. 5), resulting in a smaller overall effect of the transverse stiffness on the peak contact pressure (first panel, Fig. 5) in voice tasks targeting a specific SPL production.

The general trend of variations in voice output measures with the vertical thickness and initial glottal angle remained similar to that when all vocal fold conditions were considered in Table IV and Figs. 2 and 3. However, due to the compensatory changes in the subglottal pressure, the dependence of Qamp and MFDR on either the vertical thickness or transverse stiffness was significantly reduced so that these two measures were primarily dependent on the initial glottal angle, particularly at large initial glottal angles.

IV. DISCUSSION AND CONCLUSIONS

Previously in the study by Zhang (2019), we showed that the subglottal pressure and the transverse stiffness are the two most influential parameters on the peak contact pressure. By including conditions corresponding to a compressed initial glottal configuration, we showed in this study that medial compression also leads to significantly high contact pressure. We further showed that while the subglottal pressure and transverse stiffness can be manipulated to reduce contact pressure, such manipulations also reduce the SPL, and are thus less effective in regulating contact pressure when one aims to produce a target SPL level. In contrast, manipulations in the initial glottal angle and vertical thickness lead to changes in the contact pressure and SPL of opposite directions, i.e., changes in these two parameters that decrease the contact pressure also increase SPL. Thus, in voice tasks that demand a target SPL production, the initial glottal angle and vertical thickness can be manipulated to reduce the requirement for subglottal pressure and further reduce the peak contact pressure.

Specifically, we showed that for voice tasks that demand a target SPL, low contact pressure can be achieved with either a small and positive initial glottal angle (a barely abducted glottal configuration) or a small vocal fold thickness (e.g., head voice as opposed to chest voice). Manipulation of the initial glottal angle is the most effective at moderate target SPL levels, whereas manipulation of the vertical thickness is the most effective at high target SPL levels. Increasing the transverse stiffness (e.g., by vocal fold elongation) also has moderate effect in reducing contact pressure at high target SPL levels. For conditions in which a barely abducted glottal configuration is impossible (e.g., due to glottal insufficiency), vocal fold contact pressure can be minimized by reducing vocal fold vertical thickness and avoid compensatory increase in the subglottal pressure whenever possible. The effect of vocal fold AP stiffness on vocal fold contact pressure is relatively small.

Although similar trends were observed for both vocal tract configurations, for a given laryngeal condition and subglottal pressure, the peak contact pressure was statistically significantly higher for conditions with the /ɑ/ vocal tract than the /i/ vocal tract. On the other hand, for a target SPL level, the peak contact pressure was statistically significantly lower for conditions with the /ɑ/ vocal tract than the /i/ vocal tract, indicating that another strategy to minimize peak contact pressure is to adopt a vocal tract configuration with better source-tract impedance matching and thus a higher radiation efficiency [see, e.g., Sundberg (1974) and Titze (2006)]. This will be addressed in future studies.

While not a focus of this study, interactions between laryngeal control parameters in their effect on the peak contact pressure were observed in this study. It is possible that with a better understanding of such interactions, the peak contact pressure can be further minimized at some voicing conditions, which is worth further investigation.

The results of this study are generally consistent with findings in previous studies. For example, our study showed that the peak contact pressure reached a minimum at an initial glottal angle between 0° and 1.6°. This is similar to the 0.5 mm inter-vocal process distance (or an initial glottal angle of 1.6° assuming a 17-mm vocal fold length) at which a minimum contact pressure was observed as reported in Berry *et al.* (2001). This range of initial glottal angle appears to also correspond to the flow phonation configuration referred to in Gauffin and Sundberg (1989), which was shown to have optimal vocal acoustic efficiency. This also provides support for voice therapies that target a barely abducted glottal configuration in order to minimize vocal fold injury (Verdolini-Marston *et al.*, 1995; Peterson *et al.*, 1994). Increase in peak contact pressure at large initial glottal angles due to compensatory increase in the subglottal pressure is consistent with similar findings in Galindo *et al.* (2017).

On the other hand, the relatively large effect of the vertical thickness on the peak contact pressure observed in this study, particularly in voice tasks targeting a specific SPL level, has received less attention in the voice literature, probably due to the difficulty of *in vivo* observation of changes in the vertical thickness from a superior view. Previous studies (Hirano, 1988; Vahabzadeh-Hagh *et al.*, 2017) have shown that the vertical thickness can be increased by activation of the thyroarytenoid (TA) muscle, and reduced by activation of the cricothyroid muscle. Vocal fold thickening may also occur due to inflammation or edema. Medial compression of the membranous vocal folds necessarily involves activation of the TA muscle (Choi *et al.*, 1993; Chhetri *et al.*, 2012; Yin and Zhang, 2014), and thus changes in vertical thickness. Our results suggest that future research on vocal fold contact pressure should attempt to quantify changes in medial surface vertical thickness, or at least take it into consideration in data interpretation. This is particularly the case in human subject experiments, in which vocal fold adduction often involves simultaneous actions of both the lateral cricoarytenoid muscle, which approximates the vocal folds, and the TA muscle, which thickens the vocal folds. It is possible that targeting a barely abducted glottal configuration, as in resonant voice therapy, may also reduce TA activity and reduce the vertical thickness, which is worth future investigation.

It may be worthwhile to differentiate two mechanisms of high vocal fold contact pressure, one associated with medial compression of the vocal folds and the other associated with a large vocal fold vibration amplitude, particularly at large initial glottal angles. Our results show that aerodynamic measures (Qmean, Qamp, MFDR) appear to be effective in identifying vocal behavior with high contact pressure in conditions of large initial glottal angles (Fig. 4), but not that useful in differentiating hyperadduction conditions from optimal conditions with barely abducted vocal folds, which can be better distinguished based on CQ and voice type measures. It is possible that a set of voice features can be selected based on the findings of our study that would allow better identification and/or differentiation of vocal fold configurations with excessively high contact pressure (e.g., due to hyperadduction or glottal insufficiency) from a barely abducted vocal fold configuration with minimal contact pressure (as often targeted in voice therapy), which will be investigated in future studies.

It is generally accepted that hyperadduction leads to excessively high vocal fold contact pressure and contributes to vocal fold tissue trauma and the progressive development of vocal fold lesions such as nodules and polyps, which again leads to the requirement of higher subglottal pressure and thus higher contact pressure and further development of the vocal fold lesions (Hillman *et al.*, 1989). Our results appear to support this hypothesis. An example is given in Fig. 4 in which five progressive conditions within such a vicious cycle are labeled. Condition 1 corresponds to a barely abducted vocal fold configuration with a low vocal fold contact pressure. Condition 2 corresponds to a hyperadducted vocal fold configuration with medial compression and increased vertical thickness, which leads to a very high contact pressure and a voice characterized by a low F0, low HNR, high CQ, significantly low airflow consumption, and possibly a rough voice quality. Persistent hyperadduction behavior will lead to vocal fold tissue trauma and progressive development of vocal fold lesions, which will lead to progressively increased initial glottal angles. The presence of vocal fold lesions, especially lesions of large size, may lead to changes in vocal fold mechanical properties, glottal aerodynamics, and contact pattern that are not sufficiently described in our model. However, if we were to speculate the effect of vocal fold lesions on voice production based on the results of this study, voice production in the presence of vocal fold lesions likely leads to considerably high contact pressure on the lesion similar to that in conditions 3 and 4 in Fig. 4, with the voice characterized by a lower F0, high airflow consumption, and a reduced CQ. One way to break this cycle, other than voice rest or reduced SPL, is to adopt a thinned vocal fold geometry, as indicated by condition 5 in Fig. 4, which can be achieved through activation of the

cricothyroid muscle or weakened TA activation. The resulting voice will have a higher F0, reduced CPP and higher-order harmonics, a very low CQ, and a more regular vocal fold vibration.

In this study, vocal fold medial compression was simulated by a medial rigid-body rotation of the vocal fold with a negative initial glottal angle. As a result, maximum compression occurred by design at the posterior end of the vocal fold, whereas in reality it is more likely to occur at the mid-membranous region. The findings of this study at this negative initial glottal angle thus need to be verified in models with a more realistic implementation of medial compression of the membranous vocal folds [e.g., Wu and Zhang (2019)].

Another important limitation of our study was the neglect of the liquid layer on the vocal fold surface, which is expected to affect the dynamics of vocal fold contact and separation during phonation (Bhattacharya and Siegmund, 2014, 2015; Erath *et al.*, 2017). The peak contact pressure may be significantly reduced in the presence of this surface liquid layer, or due to viscous effects (e.g., stress relaxation) of the vocal folds. The impact of such factors should be further investigated.

ACKNOWLEDGMENTS

This study was supported by research Grant Nos. R01DC009229 and R01 DC001797 from the National Institute on Deafness and Other Communication Disorders, the National Institutes of Health. The author thanks Dr. Katherine Verdolini Abbott, Dr. Ronald Scherer, and Dr. Jody Kreiman for their valuable comments on an earlier version of this paper.

Alipour, F., Berry, D. A., and Titze, I. R. (**2000**). "A finite-element model of vocal-fold vibration," J. Acoust. Soc. Am. **108**, 3003–3012.
Alipour-Haghighi, F., and Titze, I. R. (**1991**). "Elastic models of vocal fold tissues," J. Acoust. Soc. Am. **90**, 1326–1331.
Berry, D., Verdolini, K., Montequin, D. W., Hess, M. M., Chan, R. W., and Titze, I. R. (**2001**). "A quantitative output-cost ratio in voice production," J. Speech, Lang., Hear. Res. **44**, 29–37.
Bhattacharya, P., and Siegmund, T. (**2014**). "A computational study of systemic hydration in vocal fold collision," Comput. Methods Biomech. Biomed. Eng. **17**(16), 1835–1852.
Bhattacharya, P., and Siegmund, T. (**2015**). "The role of glottal surface adhesion on vocal folds biomechanics," Biomech. Model Mechanobiol. **14**, 283–295.
Chhetri, D., Neubauer, J., and Berry, D. (**2012**). "Neuromuscular control of fundamental frequency and glottal posture at phonation onset," J. Acoust. Soc. Am. **131**(2), 1401–1412.
Choi, H., Berke, G., Ye, M., and Kreiman, J. (**1993**). "Function of the thyroarytenoid muscle in a canine laryngeal model," Ann. Otol. Rhinol. Laryngol. **102**, 769–776.
Erath, B. D., Zañartu, M., and Peterson, S. D. (**2017**). "Modeling viscous dissipation during vocal fold contact: The influence of tissue viscosity and thickness with implications for hydration," Biomech. Model Mechanobiol. **16**, 947–960.
Farahani, M., and Zhang, Z. (**2016**). "Experimental validation of a three-dimensional reduced-order continuum model of phonation," J. Acoust. Soc. Am. **140**, EL172–EL177.
Galindo, G., Peterson, S., Erath, B., Castro, C., Hillman, R., and Zanartu, M. (**2017**). "Modeling the pathophysiology of phontraumatic vocal hyperfunction with a triangular glottal model of the vocal folds," J. Speech Lang. Hear. Res. **60**, 2452–2471.
Gauffin, J., and Sundberg J. (**1989**). "Spectral correlates of glottal voice source waveform characteristics," Speech Hear. Res. **32**, 556–650.
Herbst, C., Hess, M., Müller, F., Švec, J., and Sundberg, J. (**2015**). "Glottal adduction and subglottal pressure in singing," J. Voice **29**(4), 391–402.
Hillenbrand, J. M., Cleveland, R. A., and Erickson, R. L. (**1994**). "Acoustic correlates of breathy vocal quality," J. Speech Hear. Res. **37**, 769–778.
Hillman, R., Holmberg, E., Perkell, J., Walsh, M., and Vaughan, C. (**1989**). "Objective assessment of vocal hyperfunction: An experimental framework and initial results," J. Speech Hear Res. **32**, 373–392.
Hirano, M. (**1988**). "Vocal mechanisms in singing: Laryngological and phoniatric aspects," J. Voice **2**, 1–69.
Hirano, M., and Kakita, Y. (**1985**). "Cover-body theory of vocal fold vibration," in *Speech Science: Recent Advances*, edited by R. G. Daniloff (College-Hill Press, San Diego), pp. 1–46.
Hollien, H., and Curtis, F. (**1960**). "A laminagraphic study of vocal pitch," J. Speech Hear. Res. **3**, 361–371.
Holmberg, E. B., Doyle, P., Perkell, J. S., Hammarberg, B., and Hillman, R. E. (**2003**). "Aerodynamic and acoustic voice measurements of patients with vocal nodules: Variation in baseline and changes across voice therapy," J. Voice **17**, 269–282.
Isshiki, N. (**1989**). *Phonosurgery: Theory and Practice* (Springer-Verlag, Tokyo), Chap. 3.
Jiang, J. J., and Titze, I. R. (**1994**). "Measurement of vocal fold intraglottal pressure and impact stress," J. Voice **8**(2), 132–144.
Peterson, K. L., Verdolini-Marston, K., Barkmeier, J. M., and Hoffman H. T. (**1994**). "Comparison of aerodynamic and electroglottographic parameters in evaluating clinically relevant voicing patterns," Ann. Otol. Rhinol. Laryngol. **103**, 335–346.
Story, B. H. (**1995**). "Physiologically-based speech simulation using an enhanced wave-reflection model of the vocal tract," Ph.D. dissertation, University of Iowa, Iowa City, IA, Chap. 2.
Story, B. H., Titze, I. R., and Hoffman, E. A. (**1996**). "Vocal tract area functions from magnetic resonance imaging," J. Acoust. Soc. Am. **100**, 537–554.
Sundberg, J. (**1974**). "Articulatory interpretation of the singing formant," J. Acoust. Soc. Am. **55**, 838–844.
Titze, I. (**2006**). "Voice training and therapy with a semi-occluded vocal tract: Rationale and scientific underpinnings," J. Speech Lang. Hear. Res. **49**, 448–459.
Titze, I., and Talkin, D. (**1979**). "A theoretical study of the effects of various laryngeal configurations on the acoustics of phonation," J. Acoust. Soc. Am. **66**, 60–74.
Titze, I. R. (**1995**). "Workshop on acoustic voice analysis: Summary statement," National Center for Voice and Speech, Iowa City, IA, pp. 1–36.
Vahabzadeh-Hagh, A., Zhang, Z., and Chhetri, D. (**2017**). "Quantitative evaluation of the in vivo vocal fold medial surface shape," J. Voice **31**, 513.e15–513.e23.
Verdolini K, Druker, D., Palmer, P., and Samawi, H. (**1998**). "Laryngeal adduction in resonant voice," J. Voice **12**, 315–327.
Verdolini, K., Hess, M. M., Titze, I. R., Bierhals, W., and Gross, M. (**1999**). "Investigation of vocal fold impact stress in human subjects," J. Voice **13**, 184–202.
Verdolini-Marston, K., Burke, M. D., Lessac, A., Glaze, L., and Caldwell, E. (**1995**). "A preliminary study on two methods of treatment for laryngeal nodules," J. Voice **9**, 74–85.
Wriggers, P. (**2006**). *Computational Contact Mechanics* (Springer, New York), Chap. 6.
Wu, L., and Zhang, Z. (**2016**). "A parametric vocal fold model based on magnetic resonance imaging," J. Acoust. Soc. Am. **140**, EL159–EL165.
Wu, L., and Zhang, Z. (**2019**). "Voice production in a MRI-based subject-specific vocal fold model with parametrically controlled medial surface shape," J. Acoust. Soc. Am. **146**, 4190–4198.
Yin, J., and Zhang, Z. (**2014**). "Interaction between the thyroarytenoid and lateral cricoarytenoid muscles in the control of vocal fold adduction and eigenfrequencies," J. Biomech. Eng. **136**(11), 111006.
Zhang, Z. (**2015**). "Regulation of glottal closure and airflow in a three-dimensional phonation model: Implications for vocal intensity control," J. Acoust. Soc. Am. **137**, 898–910.
Zhang, Z. (**2016**). "Cause-effect relationship between vocal fold physiology and voice production in a three-dimensional phonation model," J. Acoust. Soc. Am. **139**, 1493–1507.
Zhang, Z. (**2017**). "Effect of vocal fold stiffness on voice production in a three-dimensional body-cover phonation model," J. Acoust. Soc. Am. **142**, 2311–2321.

Zhang, Z. (**2018**). "Vocal instabilities in a three-dimensional body-cover phonation model," J. Acoust. Soc. Am. **144**(3), 1216–1230.
Zhang, Z. (**2019**). "Vocal fold contact pressure in a three-dimensional body-cover phonation model," J. Acoust. Soc. Am. **146**(1), 256–265.
Zhang, Z., and Luu, T. (**2012**). "Asymmetric vibration in a two-layer vocal fold model with left-right stiffness asymmetry: Experiment and simulation," J. Acoust. Soc. Am. **132**(3), 1626–1635.
Zhang, Z., Mongeau, L., and Frankel, S. H. (**2002**). "Experimental verification of the quasi-steady approximation for aerodynamic sound generation by pulsating jets in tubes," J. Acoust. Soc. Am. **112**(4), 1652–1663.
Zhang, Z., Samajder, H., and Long, J. (**2017**). "Biaxial mechanical properties of human vocal fold cover under vocal fold elongation," J. Acoust. Soc. Am. **142**, EL356–EL361.